Published in final edited form as:
Immunity. 2012 October 19; 37(4): 709–720. doi:10.1016/j.immuni.2012.06.021.

T Cell Affinity Regulates Asymmetric Division, Effector Cell Differentiation, and Tissue Pathology

Carolyn G. King[1,*], **Sabrina Koehli**[1], **Barbara Hausmann**[1], **Mathias Schmaler**[2], **Dietmar Zehn**[3], and **Ed Palmer**[1,*]

[1]Laboratory of Transplantation Immunology, Departments of Biomedicine and Nephrology, University Hospital Basel and University of Basel, Hebelstrasse 20, CH-4031 Basel, Switzerland [2]Laboratory of Immunoregulation, Departments of Biomedicine and Nephrology, University Hospital Basel and University of Basel, Hebelstrasse 20, CH-4031 Basel, Switzerland [3]Swiss Vaccine Research Institute, CH-1066 Epalinges, Switzerland

SUMMARY

The strength of interactions between T cell receptors and the peptide-major histocompatibility complex (pMHC) directly modulates T cell fitness, clonal expansion, and acquisition of effector properties. Here we show that asymmetric T cell division is an important mechanistic link between increased signal strength, effector differentiation, and the ability to induce tissue pathology. Recognition of pMHC above a threshold affinity drove responding T cells into asymmetric cell division. The ensuing proximal daughters underwent extensive division and differentiated into short-lived effector cells expressing the integrin VLA-4, allowing the activated T cell to infiltrate and mediate destruction of peripheral target tissues. In contrast, T cells activated by below-threshold antigens underwent symmetric division, leading to abortive clonal expansion and failure to fully differentiate into tissue-infiltrating effector cells. Antigen affinity and asymmetric division are important factors that regulate fate specification in $CD8^+$ T cells and predict the potential of a self-reactive T cell to mediate tissue pathology.

INTRODUCTION

Most T lymphocytes in an individual have a history of self-reactivity during positive selection in the thymus; they recognize proteins encoded in the major histocompatibility complex (self-MHC) and loaded with self-peptides, which are peptide fragments derived from the body's own proteins. Although positive selection promotes the development of T cells with weak self-reactivity, negative selection blocks the development of T cells with strong self-reactivity (Goldrath and Bevan, 1999b; von Boehmer et al., 1989). To generate a self-tolerant peripheral T cell repertoire, developing $CD8^+$ T cells use a specific affinity threshold for T cell receptor (TCR) binding to self-antigens to initiate negative selection (Daniels et al., 2006; Naeher et al., 2007). Although thymocytes respond to peptides over a wide range of affinities, the transition from positive to negative selection is extremely sensitive and occurs within an extremely narrow affinity range.

*Correspondence: carolyn.king@unibas.ch (C.G.K.), ed.palmer@unibas.ch (E.P.).

SUPPLEMENTAL INFORMATION

Supplemental Information include three figures and two movies and can be found with this article online at http://dx.doi.org/10.1016/j.immuni.2012.06.021.

Europe PMC Funders Author Manuscripts

The kinetics of two-dimensional TCR-pMHC interactions are important for determining how a TCR signals (Huang et al., 2010). Efficient negative selection in the thymus prevents most self-reactive high-affinity T cells from entering the peripheral repertoire but ligands at the affinity threshold induce negative selection only when expressed at sufficient concentrations. Thus, it is clear that some T cells escape thymic selection and persist in the peripheral lymphoid organs. Although escaping T cells have a threshold affinity for their target antigen and do not generally cause spontaneous autoimmunity, disease can be induced by activation with cross-reactive foreign antigens (Gronski et al., 2004; Zehn and Bevan, 2006). TCR affinity for foreign antigens is clearly a factor in the induction of autoimmunity (Gronski et al., 2004), but how this affinity relates to the selection threshold is not known. In addition, recent work by Zehn, et al. has shown that T cells with weak self-reactivity can be induced to divide and acquire effector functions after bacterial infection (Zehn et al., 2009).

In this study, we wondered how much TCR affinity is necessary for autoimmune pathology and, specifically, whether the affinity threshold established during central tolerance induction plays a role in maintaining peripheral tolerance. We found that only higher affinity, “suprathreshold” antigens (above the threshold for negative selection in the thymus) are able to induce tissue pathology. Suprathreshold ligands promoted long-lasting T cell:antigen-presenting cell (APC) contacts required for T cell polarization and asymmetric T cell division, which generates $CD8^{hi}$ proximal daughter and $CD8^{lo}$ distal daughter cells (Chang et al., 2011; Chang et al., 2007). We further showed that proximal daughters exhibited prolonged binding to antigen-loaded APCs and that such prolonged binding resulted in sustained proliferation and differentiation of these daughter cells into short-lived effector cells (SLECs). In contrast, distal daughters underwent limited proliferation and had a reduced potential to induce tissue pathology. Finally, $CD8^+$ T cells activated by low-affinity, “subthreshold” ligands (below the threshold for negative selection in the thymus) primarily underwent symmetric division, resulting in the production of progeny with shorter APC conjugation and reduced differentiation into SLECs. Taken together, these data reveal that the establishment of T cell polarity is dependent on TCR affinity and is required for the full differentiation of T cell effectors capable of initiating tissue pathology.

RESULTS

TCR Affinity Regulates the Induction of Tissue Pathology

To determine the level of self-reactivity necessary for the induction of tissue pathology, we evaluated the role of TCR affinity in mediating autoimmune diabetes. RIP-OVA mice express ovalbumin in the b cells of the pancreatic islets under the control of the rat insulin promoter (RIP) (Blanas et al., 1996). Although adoptive transfer of high numbers of naive OT-I TCR transgenic $CD8^+$ T cells specific for K^b-OVA is insufficient to induce disease, immunization with OVA peptide after OT-I T cell transfer results in rapid β cell destruction and diabetes (Behrens et al., 2004). After adoptive transfer of OT-I T cells and immunization with OVA peptide or various peptide variants (Figure S1A in the Supplemental Information available with this article online), we observed 100% diabetes induction only in response to suprathreshold (i.e., above the threshold for negative selection) antigens (Figure 1A). Diabetes induction was not simply due to the activation of high numbers of antigen-specific T cells because as few as 1.5×10^5 OT-I T cells were sufficient to induce diabetes after administration of the above-threshold peptide Q4R7 (Figure S1B). Similar to its effect in fetal thymic organ culture (Daniels et al., 2006), the T4 peptide variant exhibited threshold properties and induced diabetes in 25% of mice (Figure 1A). The below-threshold peptides Q4H7 and V4 were unable to induce diabetes in this model. These findings indicate a striking threshold effect in light of the fact that the OT-I TCR’s affinity for Q4R7-K^b is only marginally higher (<2-fold) than its affinity for Q4H7-K^b (Figure 1A) (Daniels et al., 2006).

Because antigen dose and length of presentation can affect the efficiency of $CD8^+$ T cell activation, we attempted to further boost the initial priming of transferred OT-I T cells. However, repeated immunization with the below-threshold peptide Q4H7 was unable to sufficiently immunize OT-I T cells to generate autoimmune diabetes (data not shown). Mice receiving a 10-fold higher dose of Q4H7 (500 μg) exhibited a transient increase in urine glucose, which recovered to baseline within 2 weeks. This finding suggests that activation with subthreshold antigen was unable to promote sustained effector responses (Figure S1C). Although diabetes development in RIP-OVA mice can occur independently of help from CD4 T cells, it has been reported that fewer antigen-specific $CD8^+$ T cells are required to induce disease when help from CD4 T cells is abundantly available (Hernández et al., 2002; Kurts et al., 1997). To determine whether $CD4^+$ T cell activation would enable subthreshold ligands to induce diabetes, we coinjected RIP-OVA mice with 1×10^6 B6.C-H-2-bm12 B cells, which are allogeneic for host $CD4^+$ T cells (McKenzie et al., 1979). Provision of robust $CD4^+$ T cell helper responses, however, was inefficient in converting subthreshold peptides into disease-promoting ligands (Figure 1B). In contrast, the presence of $CD4^+$ T cells increased disease incidence in T4 immunized mice (25% without versus 80% with $CD4^+$ T cell help), which highlights the threshold properties of this peptide.

To eliminate potential effects from T cell competition and to more closely mimic an endogenous T cell response, we transferred 3×10^4 OT-I T cells into RIP-OVA recipients and then induced infection with recombinant *Listeria monocytogenes* expressing either Q4R7 or Q4H7 (Lm-Q4R7 or Lm-Q4H7) (Zehn et al., 2009). Despite the presence of a highly inflammatory bacterial infection, presentation of subthreshold Q4H7 was inefficient in inducing diabetes (2/14 versus 8/8 for the above-threshold Q4R7, Figure 1C). Taken together, these data indicate that the sharp affinity threshold characteristic of central tolerance (Daniels et al., 2006; Naeher et al., 2007) is utilized by peripheral $CD8^+$ T cells with respect to the generation of peripheral-tissue pathology.

TCR Affinity Dictates the Magnitude of Effector T Cell Activation

Because Lm-Q4H7 infection was previously shown to induce T cell expansion and effector responses (Zehn et al., 2009), we next examined the ability of OVA variant peptides to activate OT-I T cells in vivo. Q4R7 peptide administration induced rapid and high surface expression of CD25, CD69, LFA-1 (CD11a), and CD8 and resulted in a vigorous proliferative response (Figures 2A-2C). In contrast, Q4H7 immunization led to much lower expression of these activation markers and stimulated less proliferation. Despite their reduced proliferation, Q4H7-stimulated OT-I T cells were able to produce interferon-γ (IFN-γ) in response to re-stimulation with OVA peptide in vitro and exhibited efficient CTL function in vivo (Figures 2D and 2E) consistent with the observations of Zehn, et al. (Zehn et al., 2009). Importantly, the magnitude of Q4R7- or Q4H7-induced effector T cell responses directly correlates with the ability of these peptides to induce T cell expansion.

T Cell Differentiation and Tissue Infiltration

High expression of CD25 promotes the development of IL-7Rα^{lo} KLRG1^{hi} short-lived effector cells (SLECs) and drives effector T cell proliferation later in the immune response (Obar et al., 2010). Indeed, *Il2ra*$^{-/-}$ $CD8^+$ T cells exhibit impaired differentiation of SLECs despite initial robust expansion. To investigate the effect of TCR affinity on SLEC differentiation in vivo, we examined the expression of IL-7Rα and killer cell lectin-like receptor G1 (KLRG1) by flow cytometry. At the peak of T cell proliferation after Listeria infection (day 6), the frequency of SLECs (IL-7Rα^{lo} KLRG1^{hi}) was higher in T cells activated by the suprathreshold peptide Q4R7 than in T cells activated by the below-threshold antigen Q4H7 (Figure 3A). This increased frequency of SLECs in Lm-Q4R7-infected mice became even more prominent at days 7 and 8 after infection, when T cell

contraction has begun to occur (Figure 3A). In contrast, the frequency of memory-precursor (MP) effector cells (IL-7Rα^{hi}KLRG1^{lo}) was decreased in mice infected with Lm-Q4R7 as compared to mice infected with Lm-Q4H7 (Figure 3A). These shifts in frequency primarily reflected an increase in SLEC numbers as a consequence of stimulation with suprathreshold Q4R7 antigen, although MPEC numbers were somewhat increased as well (Figure 3B).

The suprathreshold peptide Q4R7 also induced the upregulation of VLA-4 (also called CD49d or α4 integrin), which was maximally expressed on CD8$^+$ T cells that had undergone more than five divisions (Figure 3C). Q4H7 activated T cells did not undergo as vigorous proliferation, although the few T cells that had progressed beyond five divisions also showed increased VLA-4 expression. Interaction of VLA-4 with VCAM-1 expressed on pancreatic endothelium has been shown to regulate T cell infiltration into the pancreas (Hänninen et al., 2007). Indeed, immunization with the suprathreshold peptide Q4R7 resulted in significant islet infiltration by CD8$^+$ T cells, whereas no significant infiltration by subthreshold, Q4H7-activated T cells was observed (Figure 3D). Q4H7 induced minor infiltration late in the response at day 6, but this did not lead to any b cell loss (data not shown). Previous studies have shown that treatment with anti-VLA-4 can inhibit the homing and infiltration of antigen-specific T cells in several autoimmune models (Burkly et al., 1994; Yednock et al., 1992). To determine whether Q4R7-mediated VLA-4 upregulation was responsible for islet infiltration in RIP-OVA mice, we treated immunized mice with mAb to VLA-4 at the onset of Q4R7 priming. All control mice developed diabetes and exhibited substantial islet infiltration by CD8$^+$ T cells, whereas anti-VLA-4-treated mice remained healthy (Figures 3E and 3F). These data indicate that, despite the ability of Q4H7 to induce effector T cell responses, the scarcity of T cells expressing VLA-4 reduces islet infiltration and is therefore a limiting factor in disease development.

TCR Affinity Regulates T Cell-APC Conjugation

We wondered how the marginal affinity difference (~1.5 fold) between the Q4R7 and the Q4H7 APLs can result in such different phenotypic and functional outcomes. One of the important factors governing T cell activation is the ability of T cells to form long-lasting conjugates with APCs (Iezzi et al., 1998). Splenocyte APCs pulsed with the suprathreshold Q4R7 formed 10-fold more conjugates with OT-I T cells than did Q4H7-pulsed splenocytes (Figure 4A), which is consistent with Q4R7's ability to promote enhanced T cell proliferation. Higher concentrations of Q4H7 did not lead to increased conjugate formation (Figure 4B) or maximal expression of CD25 (Figure 4C) on OT-I T cells, even though T cell proliferation was enhanced. Despite their inability to form long-lasting interactions with APCs, OT-I T cells stimulated with subthreshold ligands are able to enter the cell cycle. They do not, however, maintain a high level of CD25 expression, which probably limits their capacity for sustained expansion (van Stipdonk et al., 2003). In contrast, above-threshold ligands such as Q4R7 induce stable conjugates, high CD25 expression, and sustained proliferation (Figures 2B, 2C, and 4A-4C).

The formation of T cell-APC conjugates is critically dependent on the TCR's ability to activate LFA-1 (Scholer et al., 2008). To examine the contribution of TCR affinity to LFA-1 activation, we incubated OT-I T cells with K^b-Q4R7 or K^b-Q4H7 tetramers and measured T cell adhesion to plate-bound purified mouse ICAM-1, the ligand for activated LFA-1. K^b-Q4R7 stimulation generated 3-fold more ICAM-1-adherent OT-I cells than stimulation with subthreshold K^b-Q4H7 (Figure 4D). This increase was mediated by LFA-1 because adhesion could be inhibited with an antibody blocking LFA-1 function. Given the importance of LFA-1-ICAM interactions for generating sustained T cell-APC contacts (Scholer et al., 2008), we next examined the effect of antigen affinity on the duration of conjugation by using time-lapse videomicroscopic imaging to track individual DC-T cell pairs. As expected, OT-I T cells formed more conjugates with Q4R7-loaded DCs than with

Q4H7-loaded DCs (11.7 ± 2.5% for Q4R7 versus 2.3 ± 0.7% for Q4H7, $p < 0.005$). In addition, OT-I-Q4R7-loaded APC conjugates were of much longer duration than OT-I - Q4H7 loaded APC conjugates (Figure 4E and Movie S1). This difference is conspicuous given the minimal difference between K^b-Q4R7 and K^b-Q4H7 in affinity for the OT-I receptor.

TCR Affinity Regulates Asymmetric Cell Division

Sustained synapses between T cells and APCs were also shown to be required for the asymmetric division of $CD8^+$ T cells responding to bacterial infection (Chang et al., 2011; Chang et al., 2007). After T cell activation, CD8 and LFA-1 redistribute to the immune synapse, and the resulting polarization sets the stage for asymmetric division, where one daughter cell (proximal [P] to the synapse) recruits greater amounts of CD8 and LFA-1 than the other (distal [D] to the synapse) (Chang et al., 2007; Dustin and Chan, 2000; Oliaro et al., 2010). To determine whether stimulation with the suprathreshold Q4R7 resulted in more asymmetric division than that with Q4H7, we transferred CFSE-labeled naive OT-I T cells into congenic recipients and followed this by immunization with peptide and LPS. After 24 to 36 hr, undivided T cells were sorted and either used directly for confocal analysis (Figure 5A) or cultured in vitro for several hours (Figure 5B) (Chang et al., 2007). A polarized distribution of CD8 was observed in Q4R7-activated mitotic T cells, which could be identified by the presence of two oppositely facing microtubule organizing centers (MTOCs). Most CD8 colocalized with only one of the MTOCs (Figure 5A, rows 1 and 2). In addition, Q4R7-generated conjoined daughter cells maintained this asymmetry; one daughter cell inherited the majority of CD8 and LFA-1 (Figures 5B and 5C). Analysis of evolutionarily conserved polarity proteins also revealed an asymmetric distribution, in that Scribble segregated to the putative proximal daughter and PKC2 segregated to the distal daughter. In addition, Numb, which is an inhibitor of Notch signaling and has a conserved role in asymmetric cell division (Betschinger and Knoblich, 2004), was preferentially localized in proximal daughter cells (Figures 5B and 5C). These findings are in agreement with the previously reported asymmetric localization of these proteins after T cell activation (Chang et al., 2011; Chang et al., 2007).

In contrast, Q4H7-activated T cells exhibited more-uniform CD8 staining prior to division (Figure 5A, rows 3 and 4), and the majority of conjoined daughter cells contained equivalent levels of synaptic proteins (CD8, LFA-1), polarity proteins (Scribble, PKCζ), and Numb (Figures 5B and 5C). A similar symmetric pattern of staining has been reported for T cells undergoing homeostatic proliferation in $Rag^{-/-}$ mice which is driven by low affinity self antigens, i.e., those that induce positive selection in the thymus (Chang et al., 2007; Ernst et al., 1999; Goldrath and Bevan, 1999a). Although Q4H7 was originally described as a strong positive selector in OT-I fetal thymic organ culture (Daniels et al., 2006), it is capable of inducing peripheral T cell proliferation (Figure 2B). However, this proliferation is more likely to result in symmetric divisions (Figures 5B and 5C) that do not fully promote effector differentiation (Figure 3).

The dependence of asymmetric division on LFA-1-ICAM interactions (Chang et al., 2007) and the inability of subthreshold ligands to induce strong LFA-1 activation, efficient conjugation, or asymmetric division (Figures 4 and 5) indicate a role for long-lasting T cell-APC contacts in regulating T cell polarity. To investigate whether prolonged T cell-APC contacts induced by high-affinity peptides are a factor in initiating asymmetric division, we examined the subcellular localization of PKCζ in dividing OT-I T cells activated by Q4R7 pulsed DCs. After 4 or 24 hr of coculture, T cell-APC conjugates were mechanically disrupted, and T cells were further cultured with LPS-activated DCs in the absence of peptide for an additional 44 or 24 hr, respectively. In-vitro-activated OT-I T cells undergoing prolonged coculture with Q4R7-loaded APCs exhibited asymmetric distribution

of PKCζ (16/19 asymmetric cells, Figure 5D). Asymmetric division correlated with higher expression of CD25 at 72 hr (Figure S2). In contrast, T cells cocultured for only 4 hr with Q4R7-pulsed DCs primarily exhibited symmetric distribution of PKCζ and correspondingly lower levels of CD25 (4/16 asymmetric cells, Figure 5D; see also Figure S2). Taken together, these data reveal a requirement for sustained contact between T cells and APCs for the establishment of T cell polarity and asymmetric division.

Asymmetric Division Promotes SLEC Differentiation and Tissue Infiltration

Asymmetric T cell division results in the generation of putative proximal and distal daughter cells with high and low amounts of CD8, respectively. The CD8 coreceptor plays a role in stabilizing TCR-pMHC interactions, and CD8 binding is required for efficient conjugation between OT-I T cells and antigen-pulsed APCs (Jiang et al., 2011; Potter et al., 2001). To investigate whether differential expression of CD8 after asymmetric division has an effect on the subsequent binding of T cells to APCs, we sorted proximal ($CD8^{hi}$) and distal ($CD8^{lo}$) daughter cells from mice primed in vivo (Figures S3A, S3B, and S3C) and cultured the sorted daughter cells with peptide-pulsed DCs. Compared to distal daughters, proximal daughters formed twice as many conjugates with 10^{-8} M peptide-pulsed APCs, a difference that increased to 6-fold at lower (10^{-10} M) antigen concentrations (Figure 6A). This suggests that proximal daughters might have a competitive advantage over distal daughters when antigen becomes limiting or when T cell competition increases, as might occur during the later expansion phase of an immune response. To examine the proliferation and phenotype of proximal and distal daughter T cells in vivo, we injected sorted proximal and distal daughter cells separately into Lm-Q4R7-infected mice that had been infected 1 day or 3 days previously. Priming of $CD8^+$ T cells in response to *Listeria* has been shown to be most efficient one day after bacterial inoculation (Pamer, 2004). Donor T cells were analyzed at days 4 and 6 after transfer. In mice infected with Lm-Q4R7 for 1 day before T cell transfer, proximal daughters exhibited a ~2.5-fold increased accumulation compared to that of distal daughters after 6 days (Figure 6B). Accumulation in proximal daughters was further increased to approximately 8-fold more than that of distal daughters in mice that had been infected with Lm-Q4R7 for 3 days prior to T cell transfer (Figure 6B). Thus, the increased accumulation of proximal daughter T cells in mice that had been infected longer (3 days) prior to T cell transfer suggests that proximal daughters continue to expand even as antigen concentrations are decreasing from the time of T cell transfer (3 days after infection) to the end point of the experiment 6 days later. In this sense, they exhibit an increased competitive fitness over distal daughters. To examine potential alterations in T cell differentiation, we identified SLEC and MPEC populations by expression of IL-7Rα and KLRG1. Six days after transfer, the ratio of SLECs to MPECs was much higher in mice that had received proximal donor T cells than in mice receiving distal donor T cells (Figures 6C and 6D). Interestingly, T cells derived from a distal daughter also exhibited a large proportion of cells expressing both KLRG1 and IL-7Rα, although the function of these cells is not known (Figure 6C). In addition, a higher proportion of the progeny of proximal daughters expanding in Lm-Q4R7-infected mice had increased expression of VLA-4 (Figure 6C).

To determine whether Q4R7-induced asymmetric cell division led to daughter cells with different potentials to induce tissue pathology, we sorted proximal ($CD8^{hi}$) and distal ($CD8^{lo}$) daughters and adoptively transferred them into RIP-OVA mice that had been infected 1 day previously with Lm-Q4R7. Although 10^4 naive OT-I T cells are less than the numerical threshold required to induce diabetes, the same number of proximal daughter cells induced diabetes in 90% (13 of 14) of Lm-Q4R7-infected mice (Figure 6E). In contrast, 10^4 distal daughter cells did not cause disease in similarly infected mice (1 of 16). It should be noted that distal daughters were able to cause disease in Lm-Q4R7-infected mice, but 5- to

10-fold higher numbers of transferred distal daughters were required to generate a similar frequency of diabetes (Figure 6E). Similarly, smaller numbers of distal daughters were sufficient to induce disease in mice infected with Lm-OVA (Figure S3D), which induced stronger and more sustained proliferation (Figure S3E).

Proximal daughters responding to Q4R7 in vitro exhibited both more proliferation and higher expression of CD25 than did distal daughters (Figure S3F). Given the importance of IL-2 signaling in SLEC differentiation, it's possible that the efficiency in SLEC differentiation shown by proximal daughters responding to Q4R7 stimulation in vivo is a result of higher CD25 expression, which in turn influences the extent of T cell proliferation. Proximal daughters responding to OVA peptide in vitro also exhibited more proliferation than distal daughters; however, CD25 expression, SLEC/MPEC ratios, and VLA-4 expression were similar in both populations (Figures S3F and S3G). It's conceivable that distal daughters can re-enter the proliferating T cell pool and differentiate into SLECs if they encounter an even higher-affinity antigen.

Taken together, these data highlight the importance of T cell expansion in causing diabetes. Although proximal daughters have a clear advantage over distal daughters in their ability to expand, transferring higher numbers of distal daughters or exposing distal daughters to the highest-affinity antigen, Lm-OVA, which elicits stronger and more sustained proliferation (Zehn et al., 2009), are sufficient to induce diabetes.

In summary, these data show that suprathreshold antigens lead to long T cell-APC contacts, asymmetric division, and the generation of polarized proximal daughter T cells. $CD8^{hi}$ proximal daughters are significantly better able to make conjugates with antigen-bearing APCs, expand, and differentiate into SLECs expressing VLA-4, a molecule required for T cell infiltration into peripheral tissues. Consistent with these observations is our finding that OT-I T cells primed with suprathreshold Q4R7 in ICAM-deficient (*Icam1*$^{-/-}$) hosts, which are unable to support asymmetric division (Chang et al., 2007), were less efficient at inducing disease after transfer into Lm-Q4R7-infected RIP-OVA mice (Figure S3H).

DISCUSSION

The experiments presented here show that an antigen affinity threshold determines the differentiated state of a responding T cell. Previous work revealed that the boundary between positive and negative selection occurs across a very sharp TCR affinity threshold (Daniels et al., 2006), but whether this affinity threshold is similarly used by peripheral $CD8^+$ T lymphocytes for the maintenance of peripheral tolerance was not previously known. Our results demonstrate that only antigens above the negative selection threshold are able to fully promote the development of effector T cells capable of infiltrating the pancreas and efficiently causing β cell destruction. It's striking that the disease-promoting ligand K^b-Q4R7 has only a marginally higher (~1.5 fold) affinity for OT-I cells than does K^b-Q4H7 (Daniels et al., 2006), which is inefficient at causing diabetes in RIP-OVA mice. This emphasizes the importance of this affinity threshold for peripheral $CD8^+$ T cell responses. That Q4R7 is an efficient negative selector (Daniels et al., 2006) underscores the importance of central tolerance in preventing highly self-reactive thymocytes from entering the peripheral repertoire.

Our data also highlight a requirement for an above-threshold antigen affinity to generate sustained T cell-APC contacts in order to maintain primary T cell expansion. ICAM-LFA-1 signals are essential for long-lasting T cell-DC conjugates (Scholer et al., 2008), and here we show that T cell activation with above-threshold ligands induces sustained T cell-APC contacts mediated by ICAM-LFA-1 interactions. Although we have not examined the

morphology of OT-I -APC synapses, a recent study (Schubert et al., 2012) demonstrates that low-affinity, autoreactive $CD4^+$ helper T cells exhibit atypical immune synapses. It would be interesting to determine whether the synapse is organized differently when a $CD8^+$ T cell recognizes a subthreshold antigen. Although ICAM-1 appears to be dispensable for the initial priming and differentiation of effector T cells, ICAM-1 deficiency results in decreased accumulation of effector T cells at later time points (Scholer et al., 2008). In addition, despite normal acquisition of effector function, LFA-1-deficient T cells were recently shown to have a specific defect in SLEC differentiation (Beinke et al., 2010). Interestingly, we observed normal cytokine production and cytotoxicity by T cells activated with below-threshold ligands. Indeed, subthreshold antigen stimulation has previously been shown to induce T cell proliferation and effector function, but the magnitude of these responses is reduced, and T cell contraction occurs earlier (Zehn et al., 2009). The earlier contraction observed in response to subthreshold activation most likely prevents the full accumulation of SLECs that mediate pancreatic β cell destruction. In this context, we observed decreased numbers of SLEC effector T cells in response to subthreshold TCR stimulation. Of note, although *Il2ra*$^{-/-}$ $CD8^+$ T cells exhibit general defects in expansion and survival after Listeria infection, the most significant decrease is observed in the SLEC subset, indicating the dependence of this population on IL-2 signaling. (Obar et al., 2010).

Importantly, our data reveal asymmetric division as an important mechanistic link between increased signal strength and T cell differentiation (Dustin and Chan, 2000). Previous work demonstrated that short stimulation leads to decreased CD25 expression and abortive clonal expansion while long stimulation promotes sustained proliferation and CD25 expression (Gett et al., 2003; van Stipdonk et al., 2003). Our data expand on these observations by showing that prematurely disrupting T cell-APC conjugates prevents asymmetric division and a concomitant increase in CD25 expression. In agreement with this, T cells primed with suprathreshold ligand in the absence of ICAM-LFA-1 signals, which are essential for long-lasting DC interactions as well as asymmetric division, are less efficient at causing diabetes when transferred into RIP-OVA mice (Chang et al., 2007; Scholer et al., 2008).

Asymmetric division results in the generation of $CD8^{hi}$ daughter cells with greater capacity than $CD8^{lo}$ daughter cells to bind antigen-loaded APCs. Higher expression of LFA-1 on $CD8^{hi}$ proximal daughters is also likely to be a factor in their enhanced conjugation with APCs (Chang et al., 2007). In vivo, these $CD8^{hi}$ daughter cells undergo enhanced proliferation, exhibit increased differentiation into SLECs and have a higher proportion of cells expressing VLA-4, which is required for tissue infiltration. Importantly, $CD8^{hi}$ proximal daughter cells are much more efficient at infiltrating peripheral tissues and inducing target cell destruction. The enhanced APC binding and differentiation of $CD8^{hi}$ proximal daughter cells reveals the importance of repeated T cell-APC encounters that occur after the onset of T cell division (Celli et al., 2005). In contrast, $CD8^{lo}$ distal daughter cells exhibited impaired accumulation of tissue-infiltrating SLECs. Interestingly, a large proportion of T cells derived from $CD8^{lo}$ distal daughters were double positive for both KLRG1 and IL-7Rα. A similar population of double-positive cells has been observed in SLP-76-deficient T cells (Smith-Garvin et al., 2010), suggesting that lower levels of T cell activation lead to incomplete or transient downregulation of IL-7Rα expression. Taken together, the data presented here suggest a scenario in which above-threshold antigens activate LFA-1 on responding T cells and lead to long-lasting conjugates and asymmetric cell division. This sequence generates $CD8^{hi}$ proximal daughter cells, which probably further upregulate CD25 expression, leading to the cells' sustained proliferation and differentiation into tissue-infiltrating SLECs.

A similar requirement for T cell polarity in SLEC differentiation was reported for both Pyk2-deficient and LFA-1 deficient T cells, which exhibit impaired SLEC differentiation

after LCMV infection (Beinke et al., 2010). Interestingly, as antigen concentrations decrease, $CD8^{hi}$ proximal daughters maintain their ability to bind strongly to antigen-bearing DCs in vitro as well as to proliferate in vivo. This contrasts with $CD8^{lo}$ distal daughters, which exhibit decreased binding to antigen-bearing DCs and decreased proliferation at lower antigen levels. These findings raise the possibility that as T cell numbers and competition for antigen increases, only above-threshold ligands are able to coordinate the polar distribution of effector fate determinants, support continued T cell expansion, and induce the acquisition of surface molecules that allow infiltration of peripheral tissues. Of note, $CD8^{lo}$ distal daughter T cells were able induce disease when 5- to 10-fold higher numbers of cells were transferred. One possible explanation is a contamination of the sorted $CD8^{lo}$ distal daughter population with a small number of $CD8^{hi}$ proximal daughter cells capable of undergoing extensive proliferation and differentiation into disease-inducing effectors. Nevertheless, distal daughters can also cause disease when transferred into RIP-OVA mice infected with Lm-OVA, which induces more sustained T cell proliferation. $CD8^{lo}$ distal daughters might be better able to respond to OVA, given the OT-I receptor's higher affinity and lower CD8 dependence for binding K^b-OVA than for binding K^b-Q4R7 (Daniels et al., 2006).

Asymmetric division also results in the unequal partitioning of the transcription factor T-bet (Chang et al., 2011; Chang et al., 2007), which is known to repress IL-7Rα expression and drive SLEC differentiation (Intlekofer et al., 2007; Joshi et al., 2007). Importantly, T-bet-deficient $CD8^+$ T cells exhibit defective effector T cell accumulation and are unable to mediate diabetes in a RIP-LCMV system (Juedes et al., 2004). Thus, in addition to differences in CD8 and LFA-1 expression, asymmetric division most likely leads to differential expression of other fate-determining factors in proximal daughters, which also promote the differentiation of tissue-infiltrating SLECs.

One general question we have not yet resolved is whether above-threshold antigens principally drive extensive T cell proliferation, which subsequently leads to asymmetric division and differentiation. Alternatively, above-threshold antigens might establish T cell polarity and asymmetric division early on in the T cell response; this initial differentiating event might propel the T cell to undergo extensive division and concomitantly acquire a SLEC phenotype.

In summary, a TCR-pMHC affinity above the negative selection threshold (K_D = 6 μM) is required for efficient induction of asymmetric division, enhanced T cell proliferation, and differentiation into SLECs capable of tissue infiltration and target cell destruction. Antigens below this affinity threshold are much less efficient at inducing asymmetric T cell division, sustaining T cell proliferation, and inducing SLEC differentiation. Finally, these data raise the question of whether autoimmunity arises when failures in thymic selection allow a small number of high-affinity, self-reactive T cells to enter the peripheral repertoire or when there is chronic stimulation of below-threshold T cells. In this respect, it's interesting that Q4H7 induces asymmetry in some OT-I T cells, which argues for the latter possibility.

EXPERIMENTAL PROCEDURES

Mice

All animal work was done in accordance with the Federal and Cantonal laws of Switzerland. Wild-type C57BL/6, C57BL/6 *Rag2*$^{-/-}$, CD45.1 congenic mice and OT-I TCR transgenic mice recognizing OVA peptide 257-264/Kb were bred in our colony. RIP-OVA mice (Behrens et al., 2004) were obtained from Jackson Laboratories (Bar Harbor, ME).

Adoptive Transfers, Immunization, and Infection with *Listeria monocytogenes*

For diabetes induction, 5×10^6 OT-I $CD8^+$ T cells were adoptively transferred intravenously into RIP-OVA mice 1 day prior to immunization with 50 mg peptide and 25 μg LPS. Urine glucose was monitored daily. Alternatively, RIP-OVA mice received 3×10^4 OT-I T cells 1 day prior to infection with *L. monocytogenes* expressing Q4R7, Q4H7, or OVA (Zehn et al., 2009). The bacteria were grown to mid-log phase, and 5,000 colony-forming units (CFUs) were then injected intravenously into mice. For confocal microscopy analysis, 5×10^6 CFSE-labeled OT-I T cells were transferred into C57BL/6 mice, and immunization with peptide and LPS followed. After 24–48 hr, undivided T cells (brightest CFSE peak) were sorted from spleens and lymph node and cultured as previously described (Chang et al., 2007).

T Cell Proliferation, Cytokine Production, and Killing Assays

OT-I $CD8^+$ T cells were labeled with 5 μM CFSE and adoptively transferred into RIP-OVA mice (5×10^6 CFSE+ T cells/mouse). One day later, mice were immunized with 50 μg Q4R7 or Q4H7 and 25 μg LPS. At day 3 after immunization, peripheral lymph nodes (axillary, inguinal, and cervical) and spleens were harvested, counted, and pooled. Fluorescence-activated cell sorting (FACS) analysis of CFSE dye dilution was used for assessment of proliferation. For the detection of intracellular cytokines, splenocytes from day-3-immunized RIP-OVA mice were stimulated with OVA peptide in vitro in the presence of monensin for 4 hr at 37°C. For assessment of CTL function in vivo, splenic APCs from CD45.1 congenic mice were labeled with 5 μM ($CFSE^{hi}$) or 0.5 μM ($CFSE^{lo}$) CFSE. $CFSE^{hi}$ and $CFSE^{lo}$ cells were pulsed for 4 hr at 37°C with 2 μM OVA or VSV peptide, respectively. Cells were mixed at a 1:1 ratio, and 10^7 APCs were injected intravenously into recipients harboring activated OT-I T cells. Surviving APCs were determined after 5 hr by flow cytometry.

T Cell Adhesion Assay

Adhesion of 1×10^6 OT-I T cells to mouse ICAM-1 was determined after stimulation with 5 μg/ml tetramer (K^bQ4R7 or K^bQ4H7) or PMA (10 ng/ml) (Mueller et al., 2004). LFA-1 blocking was carried out with 10 mg/ml CD11a mAb. T cells were incubated at 37°C for 15 min on ICAM-1-coated plates and washed so that nonadherent cells would be removed; adherent cells were then eluted and counted by Trypan blue exclusion.

Confocal Microscopy

Cells were placed on poly-L-lysine-coated coverslips (BD PharMingen), fixed with 4% formaldehyde (Polysciences), permeabilized with 0.3% Triton X-100 (Sigma) and blocked with 0.25% fish skin gelatin (Sigma) and 1% normal mouse serum. Cells were stained with anti-β-tubulin (TUB 2.1, Sigma), anti-CD8, anti-CD11a (BD PharMingen), anti-Numb, anti-Scribble, or anti-PKCζ (Santa Cruz Biotechnology). Sections of 10–15 Z stacks were acquired with a LSM 780 confocal microscope (Zeiss). Z stacks were converted into two-dimensional images, and voxel volume was calculated with Imaris Software (Bitplane). Staining was considered asymmetric when one conjoined daughter cell expressed 1.75-fold higher staining than the corresponding conjoined twin daughter cell. For immunhistochemistry analysis, pancreas sections were stained with CD8 (BD PharMingen) and insulin antibodies (Dako).

Supplementary Material

Refer to Web version on PubMed Central for supplementary material.

Acknowledgments

The authors thank L. Jeker, I. Luescher, D. Naeher, and E. Pearce for comments on the manuscript; R. Landmann for advice on culturing Listeria; E. Wagner and U. Schneider for animal husbandry; and E. Traunecker for cell sorting. The work was supported by post-doctoral grants to C.G.K. (EMBO, HSFP) and by research grants to D.Z. (310030_130512/1 [SNF]; support from Swiss Vaccine Research Institute) and to E.P. (310030B_133131/1 and Synergia [SNF], Sybilla, [EU FP7], and TerraIncognita [ERC]).

REFERENCES

Behrens GM, Li M, Davey GM, Allison J, Flavell RA, Carbone FR, Heath WR. Helper requirements for generation of effector CTL to islet beta cell antigens. J. Immunol. 2004; 172:5420–5426. [PubMed: 15100283]

Beinke S, Phee H, Clingan JM, Schlessinger J, Matloubian M, Weiss A. Proline-rich tyrosine kinase-2 is critical for CD8 T-cell short-lived effector fate. Proc. Natl. Acad. Sci. USA. 2010; 107:16234–16239. [PubMed: 20805505]

Betschinger J, Knoblich JA. Dare to be different: asymmetric cell division in Drosophila, C. elegans and vertebrates. Curr. Biol. 2004; 14:R674–R685. [PubMed: 15324689]

Blanas E, Carbone FR, Allison J, Miller JF, Heath WR. Induction of autoimmune diabetes by oral administration of autoantigen. Science. 1996; 274:1707–1709. [PubMed: 8939860]

Burkly LC, Jakubowski A, Hattori M. Protection against adoptive transfer of autoimmune diabetes mediated through very late antigen-4 integrin. Diabetes. 1994; 43:529–534. [PubMed: 8138057]

Celli S, Garcia Z, Bousso P. CD4 T cells integrate signals delivered during successive DC encounters in vivo. J. Exp. Med. 2005; 202:1271–1278. [PubMed: 16275764]

Chang JT, Palanivel VR, Kinjyo I, Schambach F, Intlekofer AM, Banerjee A, Longworth SA, Vinup KE, Mrass P, Oliaro J, et al. Asymmetric T lymphocyte division in the initiation of adaptive immune responses. Science. 2007; 315:1687–1691. [PubMed: 17332376]

Chang JT, Ciocca ML, Kinjyo I, Palanivel VR, McClurkin CE, Dejong CS, Mooney EC, Kim JS, Steinel NC, Oliaro J, et al. Asymmetric proteasome segregation as a mechanism for unequal partitioning of the transcription factor T-bet during T lymphocyte division. Immunity. 2011; 34:492–504. [PubMed: 21497118]

Daniels MA, Teixeiro E, Gill J, Hausmann B, Roubaty D, Holmberg K, Werlen G, Holländer GA, Gascoigne NR, Palmer E. Thymic selection threshold defined by compartmentalization of Ras/MAPK signalling. Nature. 2006; 444:724–729. [PubMed: 17086201]

Dustin ML, Chan AC. Signaling takes shape in the immune system. Cell. 2000; 103:283–294. [PubMed: 11057901]

Ernst B, Lee DS, Chang JM, Sprent J, Surh CD. The peptide ligands mediating positive selection in the thymus control T cell survival and homeostatic proliferation in the periphery. Immunity. 1999; 11:173–181. [PubMed: 10485652]

Gett AV, Sallusto F, Lanzavecchia A, Geginat J. T cell fitness determined by signal strength. Nat. Immunol. 2003; 4:355–360. [PubMed: 12640450]

Goldrath AW, Bevan MJ. Low-affinity ligands for the TCR drive proliferation of mature CD8+ T cells in lymphopenic hosts. Immunity. 1999a; 11:183–190. [PubMed: 10485653]

Goldrath AW, Bevan MJ. Selecting and maintaining a diverse T-cell repertoire. Nature. 1999b; 402:255–262. [PubMed: 10580495]

Gronski MA, Boulter JM, Moskophidis D, Nguyen LT, Holmberg K, Elford AR, Deenick EK, Kim HO, Penninger JM, Odermatt B, et al. TCR affinity and negative regulation limit autoimmunity. Nat. Med. 2004; 10:1234–1239. [PubMed: 15467726]

Hänninen A, Nurmela R, Maksimow M, Heino J, Jalkanen S, Kurts C. Islet beta-cell-specific T cells can use different homing mechanisms to infiltrate and destroy pancreatic islets. Am. J. Pathol. 2007; 170:240–250. [PubMed: 17200197]

Hernández J, Aung S, Marquardt K, Sherman LA. Uncoupling of proliferative potential and gain of effector function by CD8(+) T cells responding to self-antigens. J. Exp. Med. 2002; 196:323–333. [PubMed: 12163561]

Huang J, Zarnitsyna VI, Liu B, Edwards LJ, Jiang N, Evavold BD, Zhu C. The kinetics of two-dimensional TCR and pMHC interactions determine T-cell responsiveness. Nature. 2010; 464:932–936. [PubMed: 20357766]

Iezzi G, Karjalainen K, Lanzavecchia A. The duration of antigenic stimulation determines the fate of naive and effector T cells. Immunity. 1998; 8:89–95. [PubMed: 9462514]

Intlekofer AM, Takemoto N, Kao C, Banerjee A, Schambach F, Northrop JK, Shen H, Wherry EJ, Reiner SL. Requirement for T-bet in the aberrant differentiation of unhelped memory CD8+ T cells. J. Exp. Med. 2007; 204:2015–2021. [PubMed: 17698591]

Jiang N, Huang J, Edwards LJ, Liu B, Zhang Y, Beal CD, Evavold BD, Zhu C. Two-stage cooperative T cell receptor-peptide major histocompatibility complex-CD8 trimolecular interactions amplify antigen discrimination. Immunity. 2011; 34:13–23. [PubMed: 21256056]

Joshi NS, Cui W, Chandele A, Lee HK, Urso DR, Hagman J, Gapin L, Kaech SM. Inflammation directs memory precursor and short-lived effector CD8(+) T cell fates via the graded expression of T-bet transcription factor. Immunity. 2007; 27:281–295. [PubMed: 17723218]

Juedes AE, Rodrigo E, Togher L, Glimcher LH, von Herrath MG. T-bet controls autoaggressive CD8 lymphocyte responses in type 1 diabetes. J. Exp. Med. 2004; 199:1153–1162. [PubMed: 15096540]

Kurts C, Carbone FR, Barnden M, Blanas E, Allison J, Heath WR, Miller JF. CD4+ T cell help impairs CD8+ T cell deletion induced by cross-presentation of self-antigens and favors autoimmunity. J. Exp. Med. 1997; 186:2057–2062. [PubMed: 9396776]

McKenzie IF, Morgan GM, Sandrin MS, Michaelides MM, Melvold RW, Kohn HI. B6.C-H-2bm12. A new H-2 mutation in the I region in the mouse. J. Exp. Med. 1979; 150:1323–1338. [PubMed: 159937]

Mueller KL, Daniels MA, Felthauser A, Kao C, Jameson SC, Shimizu Y. Cutting edge: LFA-1 integrin-dependent T cell adhesion is regulated by both ag specificity and sensitivity. J. Immunol. 2004; 173:2222–2226. [PubMed: 15294931]

Naeher D, Daniels MA, Hausmann B, Guillaume P, Luescher I, Palmer E. A constant affinity threshold for T cell tolerance. J. Exp. Med. 2007; 204:2553–2559. [PubMed: 17938233]

Obar JJ, Molloy MJ, Jellison ER, Stoklasek TA, Zhang W, Usherwood EJ, Lefrançois L. CD4+ T cell regulation of CD25 expression controls development of short-lived effector CD8+ T cells in primary and secondary responses. Proc. Natl. Acad. Sci. USA. 2010; 107:193–198. [PubMed: 19966302]

Oliaro J, Van Ham V, Sacirbegovic F, Pasam A, Bomzon Z, Pham K, Ludford-Menting MJ, Waterhouse NJ, Bots M, Hawkins ED, et al. Asymmetric cell division of T cells upon antigen presentation uses multiple conserved mechanisms. J. Immunol. 2010; 185:367–375. [PubMed: 20530266]

Pamer EG. Immune responses to Listeria monocytogenes. Nat. Rev. Immunol. 2004; 4:812–823. [PubMed: 15459672]

Potter TA, Grebe K, Freiberg B, Kupfer A. Formation of supramolecular activation clusters on fresh ex vivo CD8+ T cells after engagement of the T cell antigen receptor and CD8 by antigen-presenting cells. Proc. Natl. Acad. Sci. USA. 2001; 98:12624–12629. [PubMed: 11606747]

Scholer A, Hugues S, Boissonnas A, Fetler L, Amigorena S. Intercellular adhesion molecule-1-dependent stable interactions between T cells and dendritic cells determine CD8+ T cell memory. Immunity. 2008; 28:258–270. [PubMed: 18275834]

Schubert DA, Gordo S, Sabatino JJ Jr. Vardhana S, Gagnon E, Sethi DK, Seth NP, Choudhuri K, Reijonen H, Nepom GT, et al. Self-reactive human CD4 T cell clones form unusual immunological synapses. J. Exp. Med. 2012; 209:335–352. [PubMed: 22312112]

Smith-Garvin JE, Burns JC, Gohil M, Zou T, Kim JS, Maltzman JS, Wherry EJ, Koretzky GA, Jordan MS. T-cell receptor signals direct the composition and function of the memory CD8+ T-cell pool. Blood. 2010; 116:5548–5559. [PubMed: 20847203]

Suzuki A, Ohno S. The PAR-aPKC system: Lessons in polarity. J. Cell Sci. 2006; 119:979–987. [PubMed: 16525119]

van Stipdonk MJ, Hardenberg G, Bijker MS, Lemmens EE, Droin NM, Green DR, Schoenberger SP. Dynamic programming of CD8+ T lymphocyte responses. Nat. Immunol. 2003; 4:361–365. [PubMed: 12640451]

von Boehmer H, Teh HS, Kisielow P. The thymus selects the useful, neglects the useless and destroys the harmful. Immunol. Today. 1989; 10:57–61. [PubMed: 2526642]

Yednock TA, Cannon C, Fritz LC, Sanchez-Madrid F, Steinman L, Karin N. Prevention of experimental autoimmune encephalomyelitis by antibodies against alpha 4 beta 1 integrin. Nature. 1992; 356:63–66. [PubMed: 1538783]

Zehn D, Bevan MJ. T cells with low avidity for a tissue-restricted antigen routinely evade central and peripheral tolerance and cause autoimmunity. Immunity. 2006; 25:261–270. [PubMed: 16879996]

Zehn D, Lee SY, Bevan MJ. Complete but curtailed T-cell response to very low-affinity antigen. Nature. 2009; 458:211–214. [PubMed: 19182777]

Europe PMC Funders Author Manuscripts

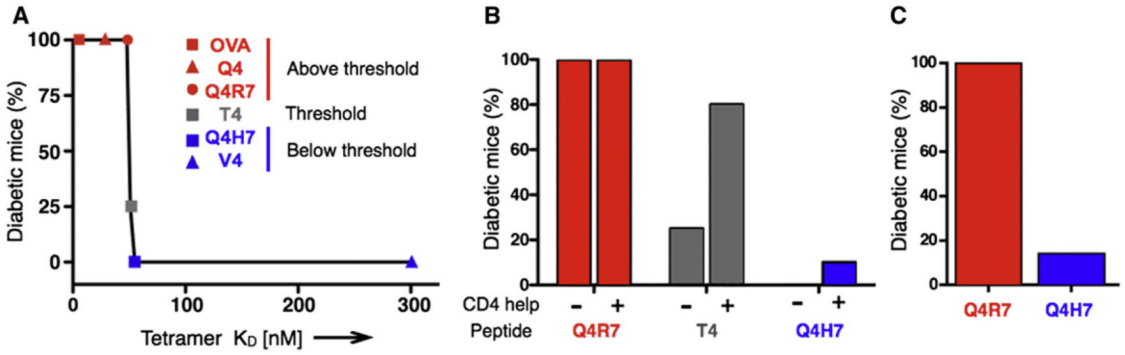

Figure 1. Incidence of Autoimmune Diabetes in RIP-OVA Mice after Immunization with High-Affinity OVA or Altered Peptide Ligands

(A) Diabetes was induced by adoptive transfer of 5×10^6 Rag-2-deficient OT-I cells into RIP-OVA mice and subsequent intraperitoneal immunization with 50 μg OVA peptide (SIINFEKL) or the indicated altered peptide ligands and 25 μg LPS (n = 5, OVA; n = 5, Q4; n = 11, Q4R7; n = 12, T4; n = 11, Q4H7; n = 5, V4). Mice were considered diabetic if urine glucose levels were ≥1000 mg/dl.

(B) Diabetes was induced as in Figure 1A with or without the addition of 1×10^6 allogeneic B6.C-H-2 bm12 B cells (n = 5, Q4R7; n = 10, T4; n = 11, Q4H7).

(C) Diabetes was induced by the adoptive transfer of 3×10^4 OT-I cells into RIP-OVA mice and subsequent infection with recombinant Lm-Q4R7 (n = 8) or Lm-Q4H7 (n = 14). (see also Figure S1). Representative data are shown of n ≥ 3 separate experiments.

Europe PMC Funders Author Manuscripts

Europe PMC Funders Author Manuscripts

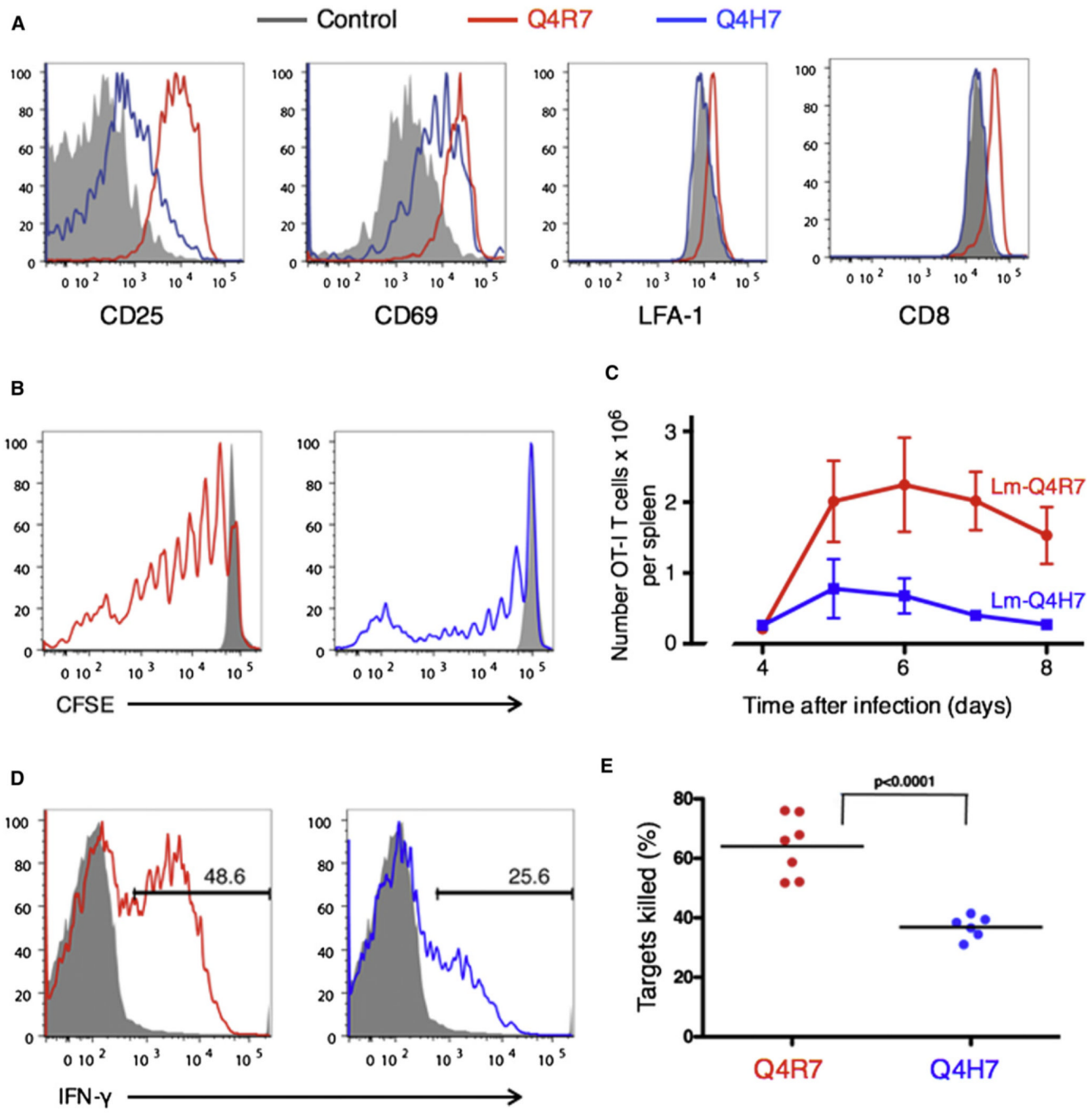

Figure 2. Characterization of In Vivo OT-I T Cell Responses after Immunization with Supratheshold or Subthreshold Peptide Ligands

RIP-OVA mice were injected with Rag-2-deficient OT-I cells, and immunization with peptide and LPS followed.

(A) Surface expression of CD25, CD69, LFA-1 (CD11a), and CD8 on lymph node OT-I T cells after 8 hr (n = 4 per peptide).

(B) CFSE dilution profiles of lymph node OT-I T cells 3 days after peptide immunization (n = 3 per peptide). The numbers of recovered OT-I donor cells from spleen and lymph nodes were equal to $2.2 \pm 0.3 \times 10^6$ and $0.7 \pm 0.1 \times 10^6$ for Q4R7 and Q4H7 immunized mice, respectively.

(C) Total numbers of splenic OT-I T cells in mice adoptively transferred with 3×10^4 OT-Is and 1 day later infected with Lm-Q4R7 or Lm-Q4H7 (two experiments, five mice per peptide).
(D) IFN-γ production by OT-I T cells restimulated for 5 hr with OVA peptide in vitro (n = 6 per peptide).
(E) CTL activity from OT-I T cells. OVA ($CFSE^{hi}$) and VSV ($CFSE^{lo}$) peptide-pulsed splenocytes were mixed at a 1:1 ratio and injected into RIP-OVA mice 3 days after peptide immunization. Target cell lysis was analyzed from splenocytes 5 hr after cell transfer. CTL activity from unimmunized mice was <10% (n = 7, Q4R7; n = 6 Q4H7). Representative data are shown for n ≥ 2 separate experiments. Error bars denote standard error of the mean (SEM).

Europe PMC Funders Author Manuscripts

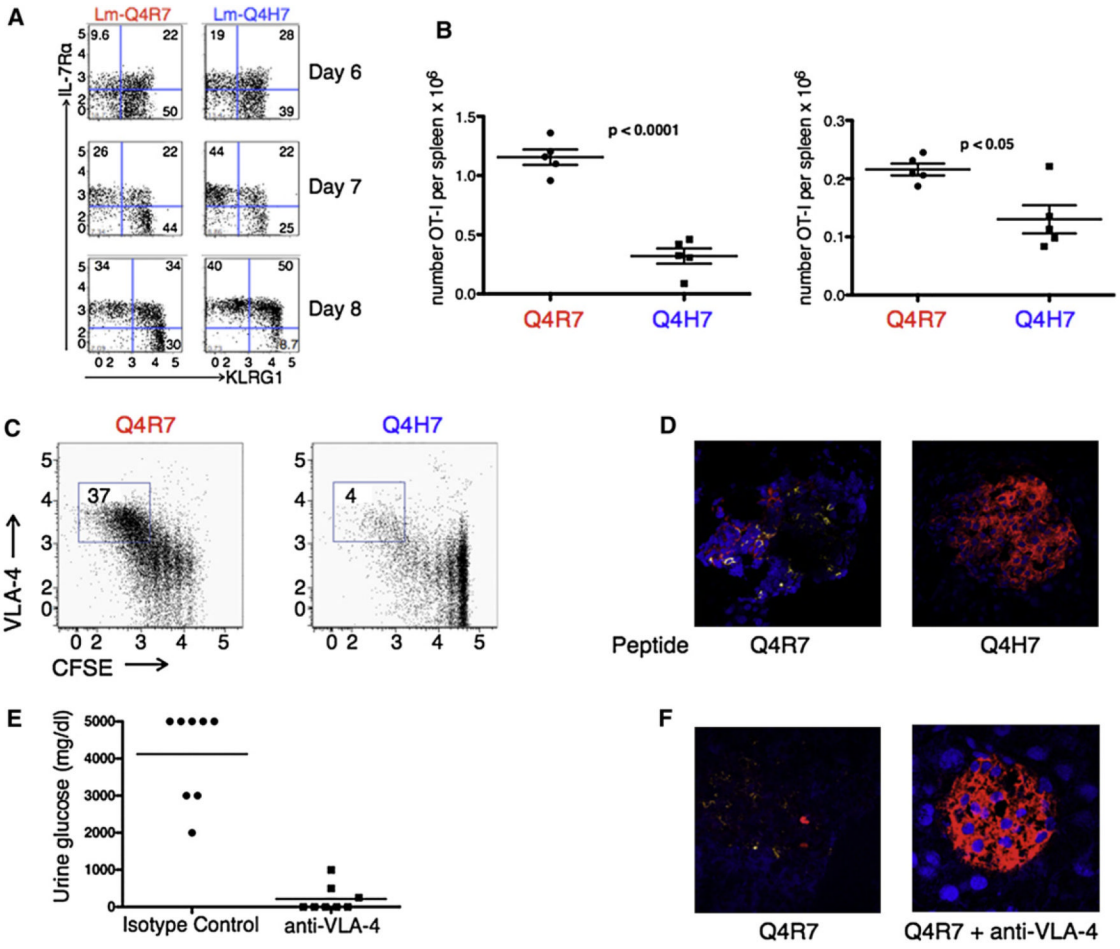

Figure 3. T Cell Differentiation and Tissue Infiltration after Immunization with Suprathreshold or Subthreshold Peptide Ligands

(A and B) OT-I T cells were adoptively transferred into C57BL/6 mice, and infection with Lm-Q4R7 or Lm-Q4H7 followed. (A) Representative flow-cytometry plots of SLEC and MPEC cells at days 6, 7, and 8 after infection. Numbers on the axes represent the log10 of fluorescence.

(B) Total splenic OT-I T cell numbers of SLEC and MPEC cells at day 6 after infection. Representative data are from two separate experiments; n = 5 mice per peptide; statistical analysis was performed with an unpaired two-tailed Student's t test. Error bars denote SEM.

(C–F) T cell infiltration and diabetes induction mediated by VLA-4 upregulation on proliferating T cells. CFSE-labeled congenic OT-I T cells (5×10^{6}) were injected into RIP-OVA recipients, and peptide immunization and LPS followed. (C) Surface expression of VLA-4 and CFSE dye dilution on LN T cells was determined at day 3. Numbers on the axes represent the log10 of fluorescence. Representative data are from two separate experiments; n = 4 mice per peptide. (D) Representative immunohistochemistry for CD8 (yellow), insulin (red), and DAPI (blue) on pancreatic sections taken 3 days after immunization; images are magnified 40× (n = 3). (E and F) Mice were treated with anti-VLA-4 (500 μg, clone PS2) or isotype control (500 μg, IgG2b) at days 0 and 2. (E) Urine glucose (n = 8) and (F) immunohistochemistry (n = 3) were examined at day 4.

Europe PMC Funders Author Manuscripts

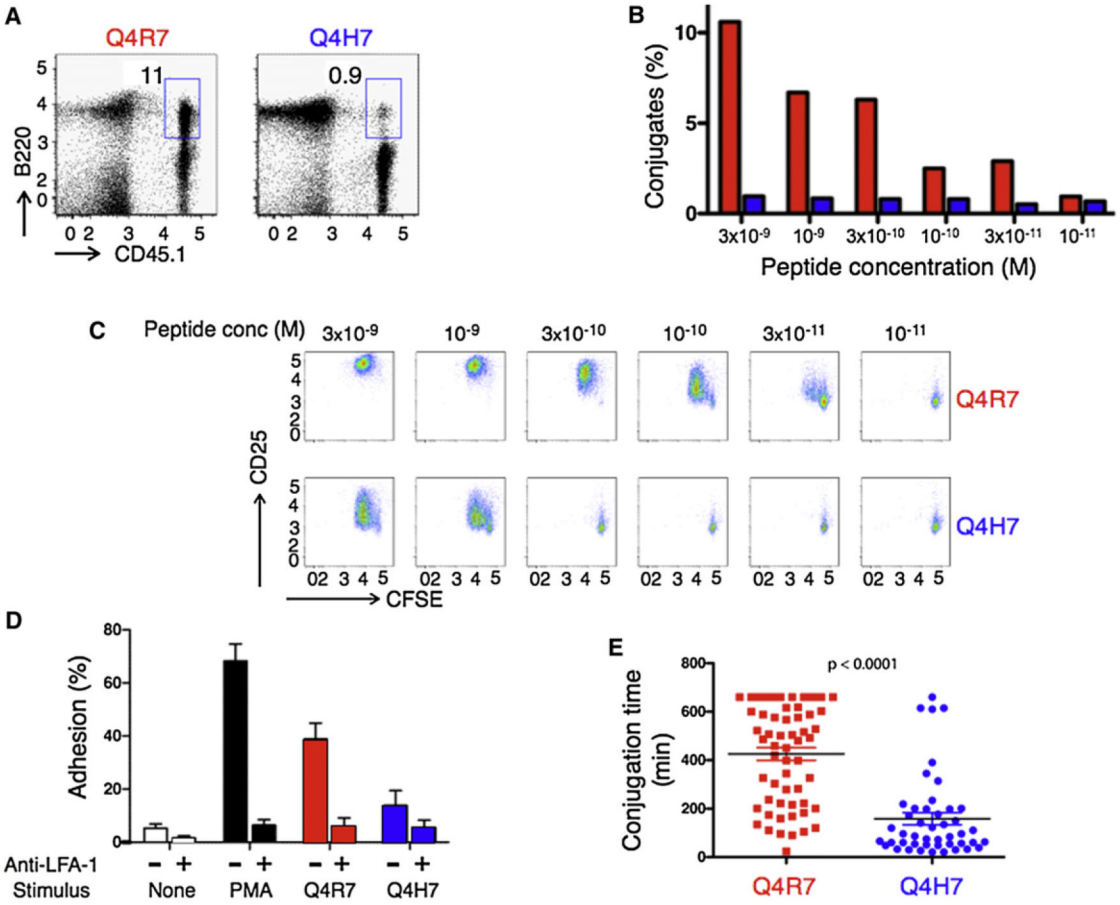

Figure 4. Conjugate Formation between OT-I T Cells and APCs Pulsed with Suprathreshold or Subthreshold Peptide Ligands

(A) APCs (C57BL/6 splenocytes) were incubated with 1×10^{-8} M peptide and LPS and mixed with congenic (CD45.1) OT-I lymphocytes. Conjugate formation was determined after antibody staining and flow cytometry. Numbers on the axes represent the log10 of fluorescence. Representative data are from four independent experiments.

(B) Splenocytes were pulsed with the indicated concentration of peptide and cultured together with OT-I T cells.

(C) Proliferation (CFSE dye dilution) and CD25 expression was assessed after 48 hr. Numbers on the axes represent the log10 of fluorescence.

(D) Adhesion of OT-I T cells to mouse ICAM-1 was determined after no stimulation or after incubation with tetramer (K^b-Q4R7 or K^b-Q4H7) or PMA (Mueller et al., 2004). Results are expressed as the mean percentage of adherent cells from triplicate wells ± SD. Representative data are from three independent experiments.

(E) Bone-marrow-derived dendritic cells were labeled with PKH-26 and incubated with 1×10^{-8} M peptide and LPS. After 4 hr, CMAC-blue-labeled OT-I T cells were added, and individual T cell-DC conjugates were tracked over a 12 hr period by time-lapse videomicroscopy. The horizontal bars indicate the average conjugation time ± SEM. Statistical analysis was performed by an unpaired two-tailed Student's t test. (see also Movie S1 and Movie S2).

Europe PMC Funders Author Manuscripts

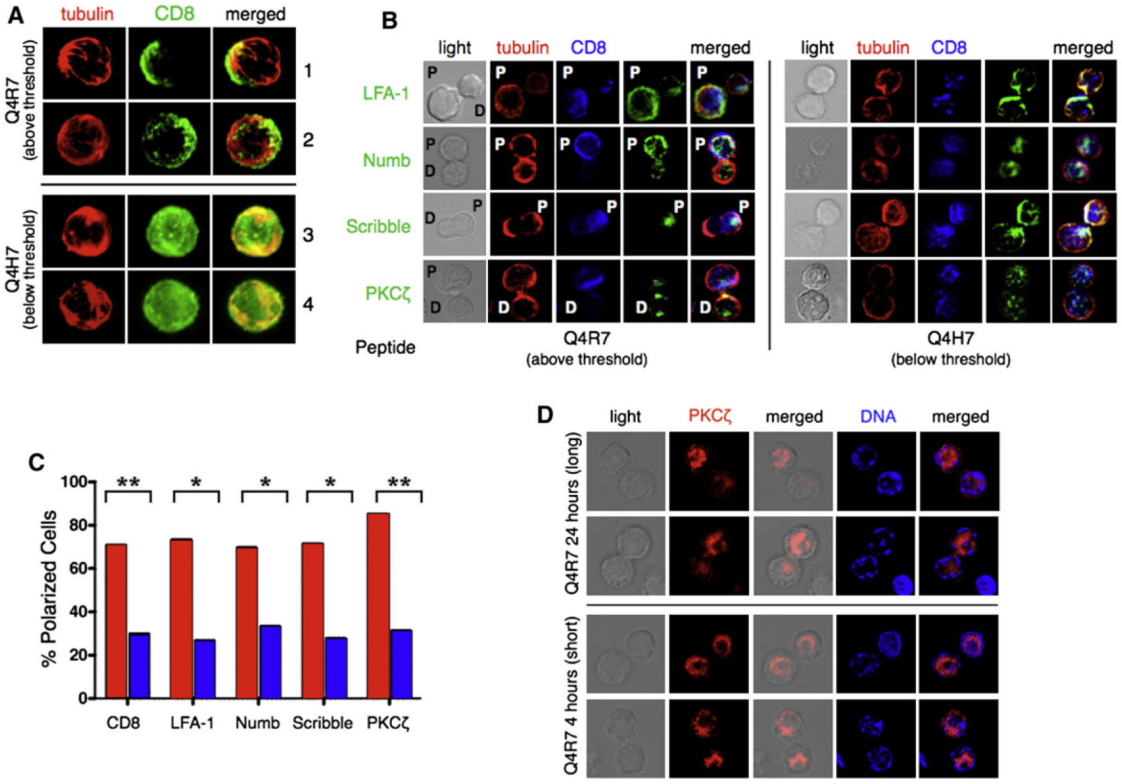

Figure 5. Assessment of Asymmetric Cell Division in OT-1 T Cells Responding to Supratheshold or Subthreshold Peptide Ligands

CFSE-labeled OT-I T cells were transferred into C57BL/6 mice, and immunization with LPS and either Q4R7 or Q4H7 followed. After 24 to 36 hr, undivided (brightest CFSE peak) OT-I T cells were sorted and analyzed by confocal microscopy for (A) β-tubulin and CD8 localization on single T cells or (B) β-tubulin, CD8, LFA-1, Scribble, Numb, and PKCζ on conjoined daughter cells (Chang et al., 2007; Oliaro et al., 2010; Suzuki and Ohno, 2006). Proximal (defined as the cell with a majority of CD8 expression) and distal daughters are marked with "P" and "D," respectively. (C) Quantification of asymmetric protein distribution in conjoined daughter T cells shown in (B). The number of conjoined daughter cells analyzed for each stain is indicated in parentheses as follows (nr Q4R7, nr Q4H7): CD8 (72, 67), LFA (15, 15), Numb (23, 18), Scribble (14, 18), and PKCζ (20, 16). *p ≤ 0.02; **p ≤ .001. Statistical analysis was performed by a two-tailed Student's t test. (D) CFSE-labeled T-1 T cells were cultured for 4 or 20 hr with Q4R7-pulsed DCs and LPS. After mechanical disruption of conjugates, T cells were purified on a magnetic column and recultured with unloaded, LPS-treated DCs for an additional 24–44 hr. Mitotic T cells were analyzed by confocal microscopy for distribution of PKCζ and CFSE (n = 19 cells, Q4R7, n = 16 cells, Q4H7) (see also Figure S2).

Europe PMC Funders Author Manuscripts

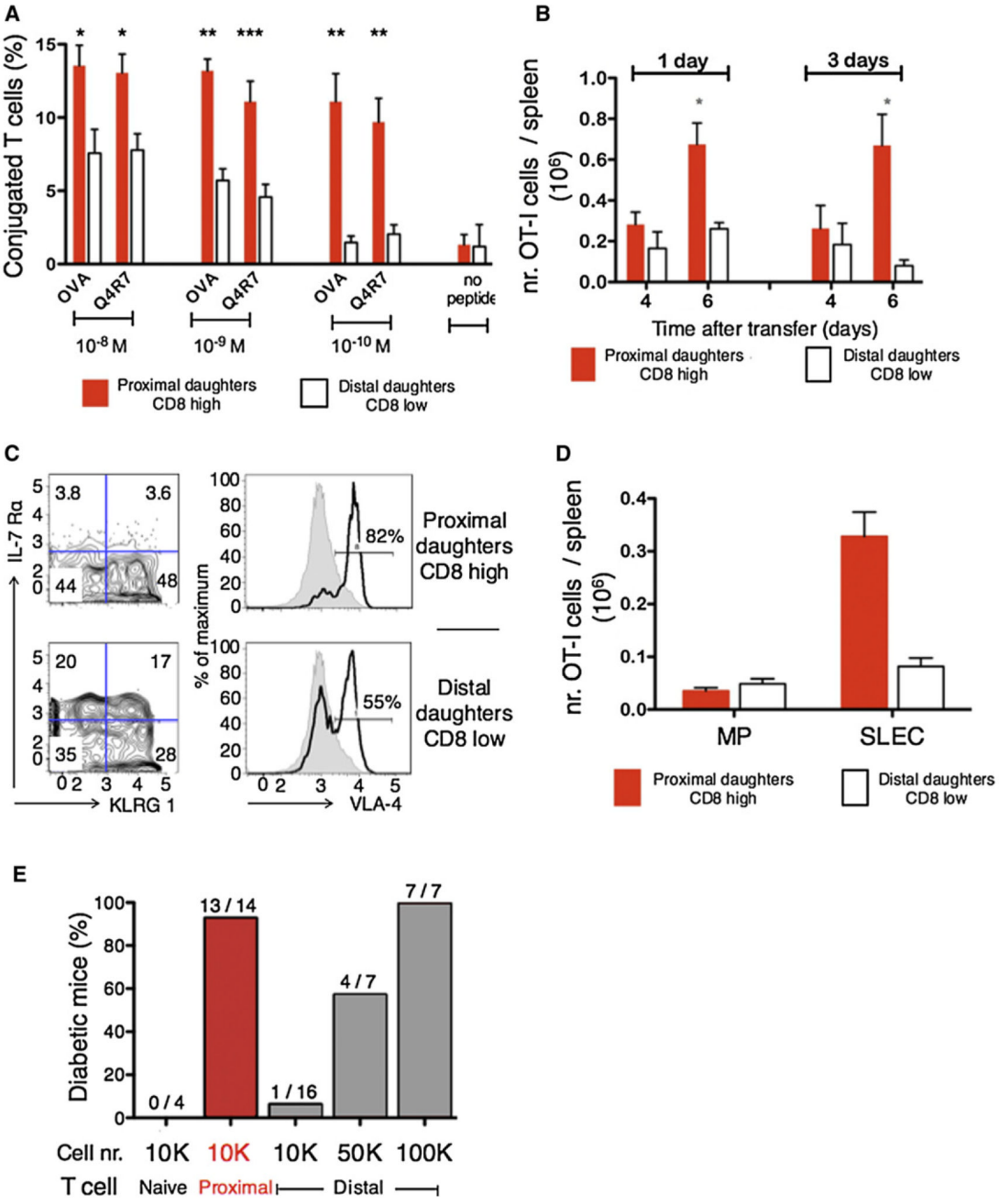

Figure 6. Phenotypic and Functional Characterization of CD8^{hi} and CD8^{lo} Daughter T Cells

CFSE-labeled OT-I T cells were injected into congenic mice, and immunization with peptide and LPS followed. After 24 hr (Q4R7), once-divided T cells (2nd CFSE peak), were sorted into CD8^{hi} (proximal daughter) and CD8^{lo} (distal-daughter) populations by FACS.

(A) Sorted T cells were cocultured with antigen-pulsed DCs, and conjugation was assessed by flow cytometry after 20 min incubation (n = 3 experiments). *p < 0.005 by an unpaired two-tailed Student's t test. Results are expressed as the mean percentage of conjugated cells ± SD.

(B–D) Sorted T cells were adoptively transferred into congenic mice that had been infected with Lm-Q4R7 1 or 3 days previously (three experiments, n = 3 mice per group). *p < 0.005. (B) Total splenic OT-I T cell numbers at days 4 and 6 after T cell transfer. (C)

Europe PMC Funders Author Manuscripts

Representative FACS plots of KLRG1, IL-7Rα, and VLA-4 6 days after T cell transfer into mice that had been infected 72 hr prior to transfer. Numbers on the axes represent the log10 of fluorescence. (D) Total splenic OT-I T cell numbers of SLEC and MPEC cells at day 6 after infection (three experiments, n = 3 mice per group). *$p < 0.001$ (unpaired two-tailed Student's t test). Results in (B) and (D) are expressed as the mean number of cells from triplicate mice ± SD.

(E) Sorted proximal or distal daughters were injected into RIP-OVA mice that had been infected with Lm-Q4R7 1 day previously. Diabetes development was assessed as in Figure 1 (see also Figures S3D and S3H).

Europe PMC Funders Author Manuscripts